molecular pharmaceutics

Article

pubs.acs.org/molecularpharmaceutics

Crystallographic Textures and Morphologies of Solution Cast Ibuprofen Composite Films at Solid Surfaces

Thomas Kellner,[†] Heike M. A. Ehmann,[†] Simone Schrank,[†] Birgit Kunert,[‡] Andreas Zimmer,[†] Eva Roblegg,[†,§] and Oliver Werzer*[,†]

[†]Institute of Pharmaceutical Sciences, Department of Pharmaceutical Technology, Karl-Franzens University Graz, 8010 Graz, Austria

[‡]Institute for Solid State Physics, University of Technology Graz, 8010 Graz, Austria

[§]Research Center Pharmaceutical Engineering GmbH, 8010 Graz, Austria

Supporting Information

ABSTRACT: The preparation of thin composite layers has promising advantages in a variety of applications like transdermal, buccal, or sublingual patches. Within this model study the impact of the matrix material on the film forming properties of ibuprofen−matrix composite films is investigated. As matrix materials polystyrene, methyl cellulose, or hydroxyl-ethyl cellulose were used. The film properties were either varied by the preparation route, i.e., spin coating or drop casting, or via changes in the relative ratio of the ibuprofen and the matrix material. The resulting films were investigated via X-ray diffraction and atomic force microscope experiments. The results show that preferred (100) textures can be induced via spin coating with respect to the glass surface, while the drop casting results in a powder-like behavior. The morphologies of the films are strongly impacted by the ibuprofen amount rather than the preparation method. A comparison of the various matrix materials in terms of their impact on the dissolution properties show a two times faster zero order release from methyl cellulose matrix compared to a polystyrene matrix. The slowest rate was observed within the hydroxyl ethyl cellulose as the active pharmaceutical ingredients (APIs) release is limited by diffusion through a swollen matrix. The investigation reveals that the ibuprofen crystallization and film formation is only little effected by the selected matrix material than that compared to the dissolution. A similar experimental approach using other matrix materials may therefore allow to find an optimized composite layer useful for a defined application.

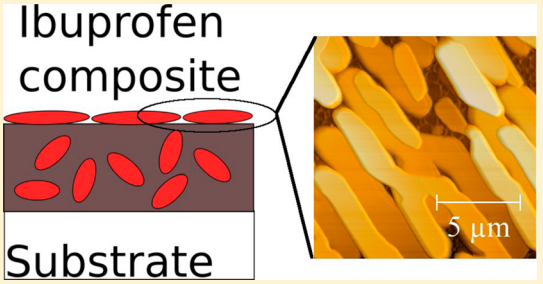

KEYWORDS: *thin film, composite, matrix, drop cast, spin cast, X-ray, texture, morphology, dissolution, release*

INTRODUCTION

The usage of administration routes other than oral provides the opportunity to apply medications that show strong degradation in the gastrointestinal tract, low solubility, and poor resorption behavior or have a first pass effect through the liver. Furthermore, patients having stomach sickness or swallow problems require other routes than oral.[1,2] The peak plasma levels of APIs can be reduced, which decreases side effects.[3,4] A promising approach is the usage of patches or thin films, which can be applied transdermal,[3,5] buccal,[6,7] or sublingual.[8] Various classes of active pharmaceutical ingredients (APIs) or drug molecules are applicable including nitroglycerine,[9] scopolamin,[10] clonidine,[11] hormones,[12] pain killers,[13] and others.

The kind of patches are manifold and strongly depend on the desired applications. For instance, single layer patches allow releasing the drug molecules without the hindrance of a matrix, while multilayers allow for retarded or multidrug formulations.[14] State of the art layers incorporate the API into a matrix , and the permeability is controlled by the epithelia barriers within or ontop of the human organism.[5] Furthermore, adhesion is required for transdermal applications[15] while within buccal or sublingual applications a dissolution of the API carrying matrix material is desired.[16,17] For patch preparations, various techniques can be applied including drop casting,[16] spin coating,[18] immersion,[19] and spray drying,[20] among others.

The preparation of patches within one process step requires a deeper understanding of the film forming properties of the composite material and the interactions of the individual components. For instance, the usage of one class of matrix material may enhance the crystallization speed, while others may even suppress crystallization allowing amorphous phases prolonging for a longer time.[21]

Within this study a model substance, ibuprofen (Ibu), is tested within three matrixes in terms of its crystalline properties and film morphologies. Ibuprofen is used as a model substance, but it is likely that it could be also applicable within sublingual or transdermal application as its distribution factor (log P) is around 4, which generally means sufficient bioavailability on these application routes.[22] The matrix materials used in this

Received: April 9, 2014
Revised: August 17, 2014
Accepted: October 2, 2014
Published: October 2, 2014

   dx.doi.org/10.1021/mp500264e | *Mol. Pharmaceutics* 2014, 11, 4084−4091

study are polystyrene, methyl cellulose and hydroxyl ethyl cellulose. While polystyrene is a good matrix, which is insoluble in water, the cellulose ethers dissolve well within aqueous environments. This means that the former would be useful within an application where the patch is removed after application. Polystyrene works well for such application,[23] but the toxicology may hinder its use in a living organism.[24,25] The celluloses are useful where a complete dissolution is desired like in buccal or sublingual applications.

For the understanding of the film forming properties of these composites, two types of deposition techniques are applied. Spin coating is a well established coating technique allowing layer thicknesses from a couple of nanometers up to hundreds of nanometers to be reproducibly prepared.[26] With drop casting also a defined layer can form, but in addition, it provides the ability to prepare much thicker films.[26] The preparation time for spin coating is shorter compared to drop casting leaving the system less time to confine in an equilibrium state, and an altered polymorph can form. Drop casting often means that components have more time to adapt favorable confinements resulting most often in favorable low energetic polymorphs.[26]

In this work, the effect of API amount with respect to the matrix on the preparation of spin-casted or drop-casted samples on a solid support (glass slides) is investigated. The samples are investigated by atomic force microscopy to identify structures at the air−sample surface interface, and the crystalline properties of the films are investigated by X-ray diffraction scans. Dissolution experiments will demonstrate the impact of the matrix material on the API release.

■ MATERIALS AND METHODS

Ibuprofen (Ibu) was provided by G.L. Pharma (Lannach, Austria). Polystyrene (PS) from Sigma (Germany) with a M_w of 100 kDa, methylcellulose (MC) from Gatt-Koller (Austria), and hydroxyethyl (HEC) from Merck (Germany) were used without further treatments. Milli-Q water, toluene (Sigma, Germany), and ethanol (Fluke, Germany) were used for the preparation of various solutions; 2 wt % PS was dissolved in toluene and 0.5 wt % MC and HEC were dissolved in a 50:50 mixture of water and ethanol. Defined amounts of Ibu were added to the matrix solutions and stirred prior use.

Samples were prepared onto conventional glass slides (Roth, Germany). The glass slides were cut in 2.5 cm squares and cleaned in ethanol solution and dried under a nitrogen stream prior to usage. The spin coating process was performed using a standard spin coater from "Ingenieurbüro Jörg Reinmuth" (Germany); to minimize the number of parameters, all samples were deposited at a rotation speed of 25 rps for 20 s. Drop-casted samples were prepared by placing a defined amount of solution (250 μL) onto glass slides, and the solvent were evaporated. All experiments were performed under ambient conditions at room temperature (23 °C).

The topography of the films was determined with a FlexAFM with an Easyscan 2 controller (Nanosurf, Switzerland) in noncontact mode. As cantilever, TAP 190 (Budgetsensors, Bulgaria) was used with a nominal resonance frequency of 190 kHz. Scans of various sizes were investigated. Data processing and data evaluation were performed with the software package Gwyddion.[27]

X-ray diffraction scans were performed with an Empyrian reflectometer (Panalytical, Netherlands). The radiation with a wavelength (λ) of 0.154 nm was provided from a copper sealed tube. A Goebbel mirror on the primary side was used for parallelizing the beam. The beam was further defined by a primary side slit system. The diffracted intensities were collected with a PixCel 3D detector. To reduce axial divergence, a soller slit was used. Within such a geometry, netplanes, which are mostly parallel to the surface, are measured; the 1D detector means that planes, which are about 1.5° inclined to the surface, are also able to contribute to the detector signal. For the data interpretation the angular measurements are recalculated to the wave vector notation (q_z) via $q_z = 4\pi \sin(\theta)/\lambda$.

Differential scanning calorimetry was performed with a Netzsch DSC 204 F1. Sample amounts of 10 mg were placed into aluminum pans by drop casting. Repeated drop casting and solvent evaporation was required to achieve the desired amount of 10 mg. Between the sample preparation and the measurements 1 week was waited allowing crystallization to be completed.

Dissolution testing was performed in glass vessels containing 50 mL phosphate buffer with a pH value of 7.2. A glass vessel was used as a standard USP apparatus would require the usage of larger samples. The buffer temperature was kept constant over the course of the experiments at 37 °C by placing the vessels into an oven. For the sake of solution convection, a stir bar was added. The dissolution experiments were performed by placing one sample into each vessel. At defined times 4 μL of the solution were withdrawn. A UV/vis spectrophotometer (Implen, NanoPhotometer) with a nanodrop attachment was used for the concentration determination. Dissolution experiments were repeated three times for better statistics.

■ RESULTS

Thermal Investigations. The DSC measurement of a pure ibuprofen sample and the ibuprofen−composite samples show the presence of a melting peak for all samples in the region between 62 to 75 °C (the extracted T_m are summarized in Table 1). The pure Ibu has a melting point at 74.3 °C in accordance with other literature values showing that the preparation of the sample in this way results in a single polymorphic structure; the polymorph with a crystal unit cell of a = 1.439 nm, b = 0.78 nm, c = 1.05 nm, and $\alpha = \gamma = 90°$ and $\beta = 99.7°$[28] has its melting point at 75.3 °C,[29] which is within errors of our investigation and is also verified via X-ray experiments (see below).

On the addition of a small amount of polystyrene, the melting point remains; in the limit of accuracy, the same. However, as the relative polystyrene content is increased, the melting of Ibu takes place at lower temperatures; at a mass ratio of Ibu−PS of 2, a T_m = 65.1 °C, and at a ratio of 1, the T_m reduced to 62.4 °C. This shows that at high PS contents, the properties of ibuprofen are slightly changed.

The same experiments performed on the composite consisting of cellulose matrix materials show a more or less independent Ibu behavior. MC or HEC in any ratio investigated did not change the melting point of Ibu at around 74 °C. The small variations present are most likely a result from sample preparation, but as the amount is low, it is very likely that ibuprofen hosted in the cellulose matrix behaves independent of its hosts.

Morphology of Spin Coating Samples. In Figure 1 the AFM height images of samples deposited via spin coating from Ibu−PS−toluene solutions with different ratios are shown. (For sake of clarity, the minimum−maximum extensions from the

dx.doi.org/10.1021/mp500264e | Mol. Pharmaceutics 2014, 11, 4084−4091

Table 1. Summary of the Samples, Their T_m Values, and the Preferred Ibuprofen Texture with Respect to the Surface for Spin or Drop Cast Films

matrix	$R_{IBU/matrix}$ (c/c)	DSC (°C)	texture		AFM height scale (nm)
			spin	drop	
PS	0.1	NA	NA	NA	30
PS	1.0	62.4	100	100	130
PS	2.0	65.1	100	powder	120
PS	3.0	74	100	powder	130
PS	4.0	73.3	100	powder	1420
PS	5.0	74.5	100	powder	750
PS	20.0	73.6	100	powder	NA
MC	0.4	72.4	100	NA	680
MC	4.0	73.4	100	100	720
MC	8.0	73.3	100	powder	780
MC	12.0	NA	100	powder	1590
MC	16.0	74.6	100	powder	1620
MC	20.0	73.5	100	powder	2100
HEC	0.4	72	100	Na	700
HEC	4.0	72.2	100	100	3390
HEC	8.0	73.5	100	powder	1900
HEC	12.0	73.2	100	powder	1400
HEC	16.0	74	100	powder	1550
HEC	20.0	73.5	100	powder	1440
IBU	pure	74.3	100	powder	NA

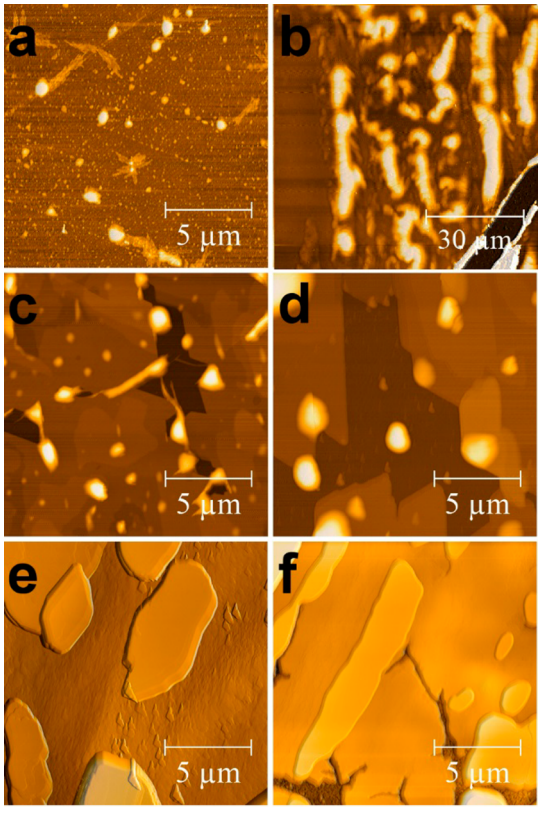

Figure 1. AFM height images of spin-coated Ibu–PS composite films with Ibu–PS mass ratio of 0.1 (a), 1 (b), 2 (c), 3 (d), 4 (e), and 5 (f).

surface are listed in Table 1.) After the spin coating process, it is expected that most of the toluene is evaporated. In addition, the samples are stored for 1 week prior to the experiments, which gives the system sufficient time to evaporate any residual solvent. At a low amount of ibuprofen the film surface shows drop-like structures with varying size and shape. In addition, the samples show more elongated structures, which are typically for crystalline Ibu.[29] Using an equal amount of Ibu and PS results in a strong deviation of the morphology with now larger elongated structures being present. A small scratch in the sample is made to reveal the average layer thickness of the sample; a line scan in this area shows an average film height of 320 nm from the surface. At a twice as large amount of Ibu with respect to the matrix, large flat structures are still present. In addition, these structures are disrupted. Assuming each plate is a single crystal of ibuprofen, this shows that in the inspected area several individual crystallites are present. The drop-like structures suggest that some of the material remained in the amorphous state; i.e., additional time would be required to crystallize all of these drop-like structures. The amount, however, is very small; thus, it can be expected that these fractions have only little or even no impact on the further experiments. A similar morphology is obtained for the sample containing three times more Ibu compared to PS. In a composite, with four or five times larger amount of Ibu, the plate-like structures are still observed but with the plates forming multiple layers on top of each other.

The morphology of samples, now prepared from Ibu–methyl cellulose (MC)–ethanol composite solutions, reveal again homogeneous films as the solutions are spin coated on to glass surfaces (see Figure 2). Compared to the film composed from Ibu and PS, the morphology at low concentrations is significantly different; the film exhibits structured particles. These particles pack closely together, like in the case of the

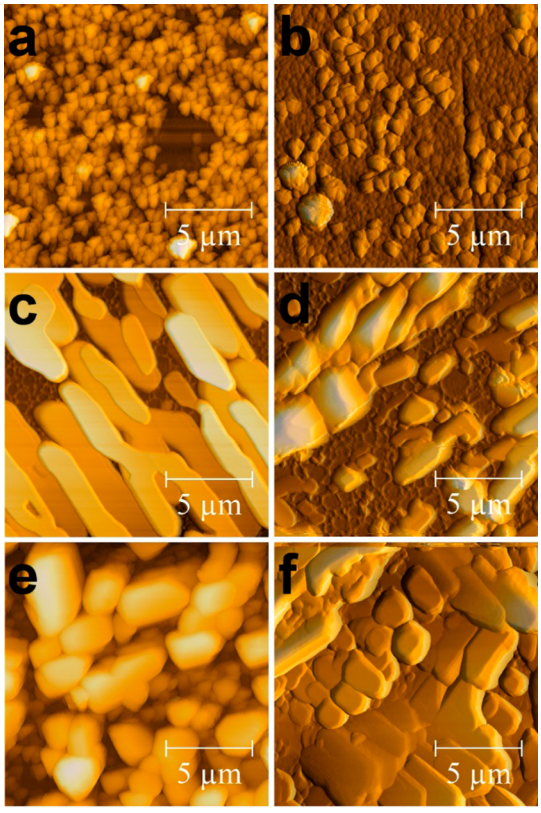

Figure 2. AFM height images of spin-coated Ibu–methyl cellulose composite films with a ratio of 0.4 (a), 4 (b), 8 (c), 12 (d), 16 (e), and 20 (f).

sample with an Ibu−MC ratio of 0.4, more separated crystallites are present (Figure 4a). Featureless drop-like structures, which are observed in Ibu−PS composites, are absent showing that full crystallization has most likely taken place. At a higher concentration (ratio of 4), most of the particles are larger, and their separation is increased (Figure 4b). In addition, smaller particles can be noted in between. This means that the preparation of such a sample results in the formation of crystalline Ibu but with the crystals having a large size distribution. More elongated plate-like structures are present for a ratio of 8. Some of these plate-like structures even show branching meaning that a single crystallite forks at some point and continuous to grow along two branches simultaneously. An increase in the relative Ibu concentration results in the lateral extension of the crystallites being reduced but with the vertical extension from the surface being increased (Figure 2d). This larger structure packs denser as the concentration is further increased (see Figure 2e,f)

The preparation of samples containing hydroxyl ethyl cellulose reveal the formation of solid surface structures (see Figure 3). At low Ibu−concentrations only some small crystals

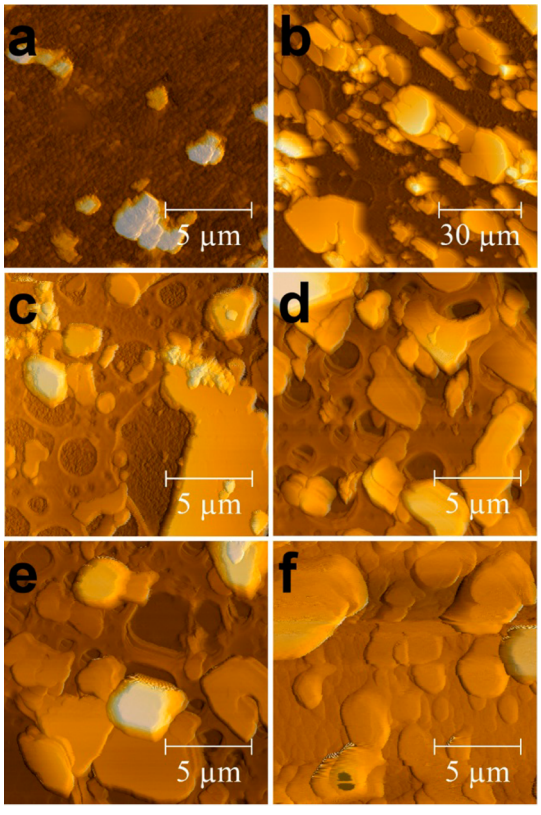

Figure 3. AFM height images of spin-coated Ibu−hydroxy ethyl cellulose composite films with a ratio of 0.4 (a), 4 (b), 8 (c), 12 (d), 16 (e), and 20 (f).

are distributed randomly over the entire surface (Figure 3a), and as the concentration is increased, more plate-like structures are noted (Figure 3b−d). Increasing the concentration further results, similar to the previous samples, in structures that have a higher extension along the surface normal (Figure 3e,f). In addition to the crystallites, which can be addressed to Ibu circular holes in the film, are noted. These holes are a consequence of the hydroxyl−ethyl cellulose, which deposited on its own already shows the formation of such structures.

Morphology of Drop-Casted Composites. The preparation of films containing Ibu and a matrix material via drop casting results in the formation of thicker films on the silica surface. In Figure 4, the AFM height images of some composite

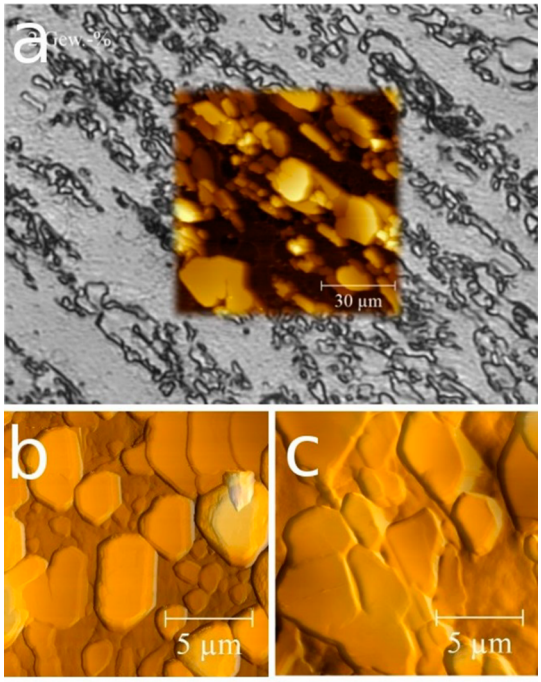

Figure 4. Combined optical micrograph and AFM height images of the drop-casted composite film containing hydroxyl ethyl cellulose (a). In the bottom row, AFM height images of polystyrene (b) and methylcellulose (c) films containing ibuprofen in a ratio of 4 with respect to the matrix are shown.

films are shown. All depicted films have a four times higher ibuprofen content compared to the matrix material. It must be noted that films prepared via a drop casting process are less homogeneous compared to films prepared from spin coating. Often large structures on the surface of the samples form, which hinder a detailed inspection of those structures with the AFM. In Figure 4 (top), an optical microscope image in bright field mode and an AFM image at the very same spot are taken and overlaid; the optical micrograph gives information on the bulk and the AFM image provides information on the surface morphology. The optical microscope shows bright areas and dark lines. The dark lines indicate the outer edges of the Ibu crystals. On a small area, homogeneous parts can be found allowing measuring the morphology with the AFM. The AFM measurements shows again the presence of a plate-like morphology within this drop-casted film.

The AFM measurements of the other samples show a similar behavior with the plate-like structure. Differences in these images are a result from poor sample position and are most likely not significant.

X-ray Diffraction Experiments. The AFM measurements reveal solid morphologies with the ibuprofen having formed large crystals during the processing at the sample surfaces. For the determination of the crystal structure and the polymorph being present in the samples, specular X-ray diffraction experiments are performed, and the results are depicted in Figure 5. The measurement of the X-ray pattern of the sample containing the lowest amount of Ibu hosted in the PS matrix

dx.doi.org/10.1021/mp500264e | *Mol. Pharmaceutics* 2014, 11, 4084−4091

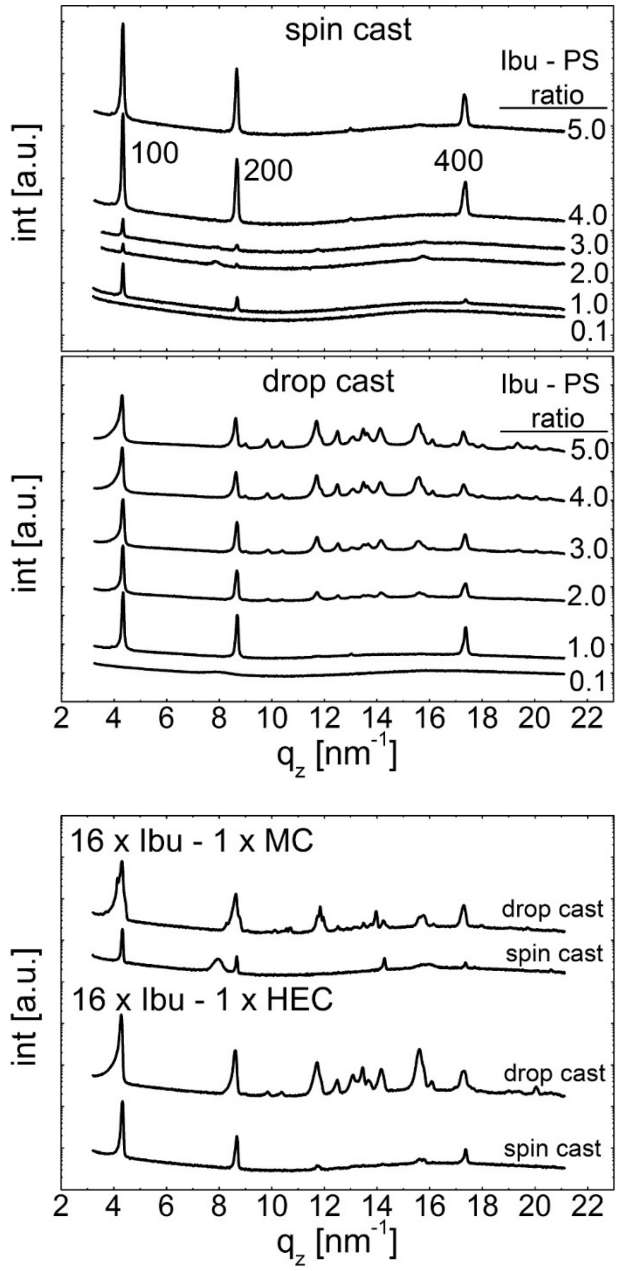

Figure 5. Specular X-ray diffraction patterns of the various composite samples containing different ratios of ibuprofen and polystyrene. The lower diagram shows selected measurements of cellulose (MC and HEC) composites prepared via spin coating or drop casting for one concentration.

results in no peaks being visible within the scan independent of the preparation method. This means that the amount of Ibu is too low to be detected by the experimental setup in use. Anyway increasing the amount of Ibu so that the ratio with the matrix is 1, i.e., the amount of both is the same, 3 peaks are noted. The peak position are at 4.35, 8.70, and 17.4 nm^{-1} showing that this peak series is a result of one netplane series, i.e., with the 100 reflection, and its higher orders (200 and 400). Again this behavior is independent of the preparation method. The 300 reflection is absent in accordance with the known crystal structure with the monoclinic unit cell, a = 1.439 nm, b = 0.78 nm, c = 1.05 nm and $\alpha = \gamma = 90°$ and $\beta = 99.7°$ in the space group $P21/c$.[29]

Increasing the amount of Ibu further, so that a twice as high amount of Ibu is present in the sample, has no effect on the X-ray pattern of the spin-coated samples. However, in the X-ray pattern of the drop-casted sample, additional peaks appear within the spectra. The peak position is located in between the 200 and 400 reflection, i.e., between 8.7 and 17.4 nm^{-1}. These various peaks correspond again to Ibu in the same polymorphic structure with 210, 012, and 202 being the most prominent peaks. This shows that in the drop-casted samples at higher Ibu loads a preferred orientation is absent and crystal formations in more random arrangements take place. Increasing the Ibu−PS ratio further results in the peak intensities being increased, which agrees well with an increase in the amount of Ibu in the sample but with the preferred textures in the spin-coated and the powder-like character in the drop-casted film prevailing.

Similarly, the usage of the other matrix materials does not significantly change this behavior. Exemplary X-ray patterns of a spin-coated and a drop-casted MC sample are shown in Figure 5 (bottom). Again the spin-coated samples show a preferred orientation with a mainly 100 texture, and a powder-like characteristic is found for the drop-casted samples. Using a HEC matrix prevails this characteristic. Within some of the X-ray patterns low intensity peaks besides the H00 series are noted showing that the 100 texture is slightly disrupted for some crystallites, but as the intensity is low, it can be concluded that this crystallites are a minority species. Additional X-ray data for other samples with varying Ibu concentration are provided in the Supporting Information.

Dissolution Testing. The release of the API from the samples is determined by dissolution experiments in Milli-Q water. The amount of drug dissolved as a function of time for three samples all containing the same amount of Ibu but differing in their matrix material is plotted in Figure 6. For the

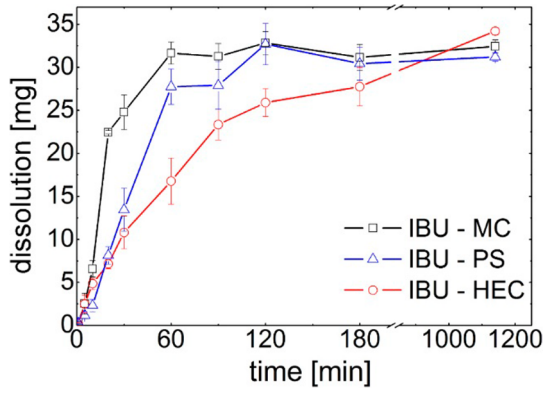

Figure 6. Ibuprofen dissolution from the various matrix material as a function of time. All samples contain a 20 times higher ibuprofen content compared to the matrix material and were prepared via drop casting. Lines are for eye guidance only.

sample made from MC, the increase of the API amount at short times is very strong with 22.5 mg being released after 20 min (see squares in Figure 6). After this first drug burst, the rate at which the API is released decreases, and after 60 min, most of the ibuprofen is dissolved. The sample containing the PS matrix shows a similar dissolution profile but with the rate at the beginning being lower compared to the MC sample (triangles in Figure 6). The released Ibu amount is very similar to the MC sample after and is about 30 mg.

The dissolution behavior of the sample consisting of the HEC matrix deviates significanlty from the two others with the rate being the slowest. This results in the API dissolution taking much longer, and even after 180 min dissolution time, the API concentration in the buffer increases. At a time of 1140 min, the last measurement was taken and a slightly higher amount of the API is dissolved compared to the others; 34.1 mg was dissolved from the HEC matrix, while the MC matrix and the PS matrix allowed the release of 32.4 and 31.2 mg, respectively, over this period of time even though the mass amount of Ibu is the same within each sample.

DISCUSSION

Pure ibuprofen is an API that requires a long time for crystallization as it is deposited onto the glass slides (see Supporting Information). The evaporation of the solvent results in a solvent free film in which the molecules adapt a random conformation (amorphous state). In addition, Ibu is delivered as a racemic mixture, which means that the sterical arrangement of the carbon acid can vary. The molecules are also asymmetric, which follows that crystallization rotational and translation arrangements have to take place before the molecules are able to pack into a low energetic crystalline state. Even the formation of a stable nuclei is disfavored by these facts. The addition of a matrix material like PS assists in nucleation, and crystallization completes after a significantly shorter time. Ibu deposited on glass requires at least 14 days at ambient condition to transfer into a crystalline state, while the presence of PS allows adapting such a crystalline arrangement within 1 day (see Supporting Information). Some residual amorphous fractions may still be present, but after 5 days, no more significant changes of the crystalline properties can be observed within an X-ray experiment. This is independent of the matrix material, and a very similar behavior exists in the samples containing cellulose. A miscibility of the two components on the molecular level can be excluded for the samples as the melting temperature remains very similar, independent of the Ibu concentration. Only within the samples containing the smallest Ibu amount in a PS matrix results in a shift of the T_m. This is most likely a result of PS and Ibu having a relatively large connecting surface area. PS is known to have a T_g that changes with layer thickness.[30,31] Within a composite, fractions of Ibu and PS alter. Small portions may therefore behave like a thin film influencing the properties of the Ibu in its vicinity.

The investigation of the various samples prepared either via spin casting or drop casting shows many similarities. First of all, the surface structure strongly changes as the Ibu concentration is changed. At low concentrations, small structures are noted while, increasing Ibu concentrations results in large surface structures. As the X-ray investigations show a unique crystal polymorph is present, for all samples investigated, these surface structures must be a result of Ibu crystallizing at the surface. From the experiments, it cannot be decided if the crystallization is a result from Ibu within the matrix inducing such crystallization or if the structures are a result from crystallized Ibu sitting on top of the matrix. Anyway, a certain amount of the Ibu can be expected to be located within the matrix as the dissolution profiles of the various samples should be more alike in the case of all Ibu sitting on top.

A comparison of these results with literature shows that the resulting surfaces may be a result from convection driven processes.[29] For instance, at low evaporation rates of EtOH from calcium stearate pellets, the material is dragged to the surface as the liquid travels to the surface to get evaporated. Repeating this process at elevated temperatures results in the Ibu distribution within the pellet being more homogeneous. It is very likely that the investigated structures in this study are a result from a similar behavior; the Ibu is dragged to the composite−air interface as the solvents evaporate. As both types of samples, i.e., spin coated and drop casted, show very similar behavior, it can be concluded that formation of the composite layers behaves independent of the methods used indicating that both methods are slow in terms of a convection process.

The preparation of the spin-coated samples show a preferred alignment of Ibu with respect to the surface; the X-ray investigations reveal the 100, and its higher order reflections are the most prominent. Some other peaks are also noted for some samples, but as the relative peak intensities are low, it can be conclude that this is a minority fraction. A random powder should reveal higher intensities for peaks other than the H00 series. In fact, the drop-casted samples show a powder-like characteristic with various relatively intense peaks being distributed over the entire spectra.

The differences in the preparation technique may be the reason for their crystallographic differences. Spin coating results in thin layers (about 300 nm in this study), while drop-casted samples are much thicker (typically 10−100 times). The matrix materials provide holes in which Ibu is hosted. As an enclosure means many surfaces are present, nucleation can take place in an abritratry direction resulting in the orientation of the crystallites being also arbitrary. This results in a powder-like characteristic observed in the specular X-ray diffraction scans of the drop-casted films. Spin-coated samples may be just too thin, for the bulk being able to contribute to the diffraction signal or crystallization along certain directions is limited or hindered.

On the free surface, crystallization is not limited by a surrounding enclosure, and large plate-like structures result. A preferred orientation may therefore easier accessible. From the experiments, however, it can not unambiguously followed which orientation is present at the surface. Obviously plate-like structures are present, which together with the strong H00 reflections in the X-ray spectra may suggest that the upper surface of the crystallites correspond to this plane.

The dissolution experiments reveal differences of the API release dependent on the matrix material. Using a MC matrix, a high dissolution rate is noted, while HEC retards the Ibu release. A detailed inspection of the dissolution curve in Figure 6 shows that a linear increase of the dissoloved API amount is present for the MC and the PS sample at the beginning; a slope of 1.36 is determined for the MC sample and 0.52 for the PS sample. A linear increase represents a zero order release meaning that at each time interval the same amount of Ibu is released into the dissolution media. The release from the MC matrix is about double as fast compared to the PS matrix. The dissolving MC matrix most likely allows the exposure of more Ibu surface area to the Milli-Q water, which according to the Whitney−Noley equation means faster dissolution. Within the insoluble PS matrix, open pores are likely present, but the surface area accessible for the dissolution media is smaller compared to the disintegrating MC matrix; thus, a slower dissolution is observed.

The dissolution behavior of the HEC samples are distinct from the other two, and a nonlinear time dependence is present. Via plotting the square root of the time vs the

dx.doi.org/10.1021/mp500264e | Mol. Pharmaceutics 2014, 11, 4084−4091

dissolution shows a linear behavior (see Supporting Information), which accordingly to the simplified Higuchi model ($M/M_\infty = k_0 t^{1/2}$)[32] means that the dissolution is limited by a diffusion process. As the HEC swells on the first contact with water rather than dissolving, the API has to diffuse through the swollen matrix to be able to transit into the dissolution media. Thus, a retarded drug release is observed.

The AFM measurements show clearly surface structures, which are expected to result in a similar dissolution being present at the beginning of the experiment. However, the dissolution curve significantly differs over the entire dissolution experiment suggesting that the surface structure does not effect the overall dissolution behavior. The amount of surface bound material may be too low to actually have a large impact, or the effect of the surface is just not accessible in the time intervals chosen for the dissolution experiment, meaning that within the first data point an immediate release has taken place leaving a free surface (without Ibu) for the further experiments.

The three types of matrix material show a significant difference in their dissolution behavior. The materials were chosen as they promise application-relevant properties, i.e., the insoluble PS matrix could be used in a transdermal usage, while the others are applicable in buccal or sublingual patches. However, the dissolution tests were performed in Milli-Q water to simplify their direct comparison. More physiological dissolution media may result in completely different dissolution properties which may justify their usage or rejection. Other matrix materials like chitosan, PLGA, or others were not tested, but it can be expected that a similar approach can be applied to such matrix materials, which would allow for identifying the best API−matrix combination for an application within a living organism.

CONCLUSIONS

The preparation of the composite materials including Ibu shows a variety of morphological and structural changes. The preparation procedure has a decisive impact on the crystal orientation with spin coating resulting in mainly 100 texture and the drop casting showing a powder-like characteristic. Besides the type of preparation, the amount of Ibu with respect to the matrix material has a strong impact on the resulting film morphology. At low concentrations, small surface structures are present, and at high concentrations, the structure sizes increase. Surprisingly, a strong impact of the matrix material on the Ibu crystallization is only evident at low concentrations. At high concentrations, similar morphologies form independent of the matrix. The dissolution experiments show a strong influence of the matrix material on drug release with the PS and MC samples showing a zero order release, and the HEC matrix retards the Ibu dissolution. It can be expected that composite formation can be achieved using other matrix materials with similar morphological and crystallographic properties. Most likely these will differ in their dissolution properties.

ASSOCIATED CONTENT

Supporting Information

Specular X-ray diffraction scans. This material is available free of charge via the Internet at http://pubs.acs.org.

AUTHOR INFORMATION

Corresponding Author

*E-mail: oliver.werzer@uni-graz.at.

Notes

The authors declare no competing financial interest.

ACKNOWLEDGMENTS

The work was funded by the Austrian Science Fund (FWF): [P25541-N19].

REFERENCES

(1) Nachum, Z.; Shupak, A.; Gordon, C. R. Transdermal scopolamine for prevention of motion Sickness. *Clin. Pharmacokinet.* **2006**, *45* (6), 543−566.

(2) Van Marion, W.; Bongaerts, M.; Christiaanse, J.; Hofkamp, H.; Van Ouwerkerk, W. Influence of transdermal scopolamine on motion sickness during 7 days' exposure to heavy seas. *Clin. Pharmacol. Ther.* **1985**, *38* (3), 301−305.

(3) Kusum Devi, V.; Saisivam, S.; Maria, G.; Deepti, P. Design and evaluation of matrix diffusion controlled transdermal patches of verapamil hydrochloride. *Drug Dev. Ind. Pharm.* **2003**, *29* (5), 495−503.

(4) Lawson, G. M.; Hurt, R. D.; Dale, L. C.; Offord, K. P.; Croghan, I. T.; Schroeder, D. R.; Jiang, N. S. Application of serum nicotine and plasma cotinine concentrations to assessment of nicotine replacement in light, moderate, and heavy smokers undergoing transdermal therapy. *J. Clin. Pharmacol.* **1998**, *38* (6), 502−509.

(5) Mukherjee, B.; Mahapatra, S.; Gupta, R.; Patra, B.; Tiwari, A.; Arora, P. A comparison between povidone-ethylcellulose and povidone-eudragit transdermal dexamethasone matrix patches based on in vitro skin permeation. *Eur. J. Pharm. Biopharm.* **2005**, *59* (3), 475−483.

(6) Nafee, N. A.; Boraie, M.; Ismail, F. A.; Mortada, L. M. Design and characterization of mucoadhesive buccal patches containing cetylpyridinium chloride. *Acta Pharm.* **2003**, *53* (3), 199−212.

(7) Guo, J.-H. Bioadhesive polymer buccal patches for buprenorphine controlled delivery: formulation, in-vitro adhesion and release properties. *Drug Dev. Ind. Pharm.* **1994**, *20* (18), 2809−2821.

(8) James, I. G.; O'Brien, C. M.; McDonald, C. J. A randomized, double-blind, double-dummy comparison of the efficacy and tolerability of low-dose transdermal buprenorphine (BuTrans Seven-Day Patches) with buprenorphine sublingual tablets (Temgesic) in patients with osteoarthritis pain. *J. Pain Symptom Manag.* **2010**, *40* (2), 266−278.

(9) Cowan, J. C.; Bourke, J. P.; Reid, D. S.; Julian, D. G. Prevention of tolerance to nitroglycerin patches by overnight removal. *Am. J. Cardiol.* **1987**, *60* (4), 271−275.

(10) Tigerstedt, I., Scopolamine. In *Transdermal Fentanyl*; Springer: New York, 1991; pp 195−200.

(11) Shah, V. P.; Tymes, N. W.; Skelly, J. P. In vitro release profiles of clonidine transdermal therapeutic systems and scopolamine transdermal patches. *Pharm. Res.* **1989**, *6* (4), 346−351.

(12) Samsioe, G. Transdermal hormone therapy: gels and patches. *Climacteric* **2004**, *7* (4), 347−356.

(13) Kornick, C. A.; Santiago-Palma, J.; Moryl, N.; Payne, R.; Obbens, E. A. Benefit-risk assessment of transdermal fentanyl for the treatment of chronic pain. *Drug Safety* **2003**, *26* (13), 951−973.

(14) Waghulde, S.; Naik, P.; Gorde, N.; Juvatkar, P.; Shirodkar, P.; Kale, M. Development, recent inventions and evaluation techniques of transdermal drug delivery system: A review. *Int. J. Pharm. Phytopharmacol. Res.* **2013**, *3* (2), 152−160.

(15) Guyot, M.; Fawaz, F. Design and in vitro evaluation of adhesive matrix for transdermal delivery of propranolol. *Int. J. Pharm.* **2000**, *204* (1), 171−182.

(16) Vishwkarma, D.; Tripathi, A.; Yogesh, P.; Maddheshiyab, B. Review article on mouth dissolving film. *J. Global Pharm. Technol.* **2011**, *3* (1), 1−8.

(17) Venkatalakshmi, R.; Sudhakar, Y.; Madhuchudana Chetty, C.; Sasikala, C.; Varma, M. Buccal drug delivery using adhesive polymeric patches. *Int. J. Pharm. Sci. Res.* **2012**, *3* (1), 35−41.

(18) Jin, C. Y.; Han, M. H.; Lee, S. S.; Choi, Y. H. Mass producible and biocompatible microneedle patch and functional verification of its usefulness for transdermal drug delivery. *Biomed. Microdevices* **2009**, *11* (6), 1195−1203.
(19) Cormier, M.; Johnson, B.; Ameri, M.; Nyam, K.; Libiran, L.; Zhang, D. D.; Daddona, P. Transdermal delivery of desmopressin using a coated microneedle array patch system. *J. Controlled Release* **2004**, *97* (3), 503−511.
(20) Gill, H. S.; Prausnitz, M. R. Coated microneedles for transdermal delivery. *J. Controlled Release* **2007**, *117* (2), 227−237.
(21) Jain, P.; Banga, A. K. Inhibition of crystallization in drug-in-adhesive-type transdermal patches. *Int. J. Pharm.* **2010**, *394* (1), 68−74.
(22) Cilurzo, F.; Minghetti, P.; Casiraghi, A.; Tosi, L.; Pagani, S.; Montanari, L. Polymethacrylates as crystallization inhibitors in monolayer transdermal patches containing ibuprofen. *Eur. J. Pharm. Biopharm* **2005**, *60* (1), 61−66.
(23) Ehmann, H. M.; Zimmer, A.; Roblegg, E.; Werzer, O. Morphologies in solvent annealed clotrimazole thin films explained by Hansen-solubility parameters. *Cryst. Growth Des.* **2014**, *14*, 1386−1391.
(24) Fröhlich, E.; Meindl, C.; Roblegg, E.; Griesbacher, A.; Pieber, T. R. Cytotoxity of nanoparticles is influenced by size, proliferation and embryonic origin of the cells used for testing. *Nanotoxicology* **2012**, *6*, 424−439.
(25) Roblegg, E.; Frohlich, E.; Meindl, C.; Teubl, B.; Zaversky, M.; Zimmer, A. Evaluation of a physiological in vitro system to study the transport of nanoparticles through the buccal mucosa. *Nanotoxicology* **2012**, *6* (4), 399−413.
(26) Wedl, B.; Resel, R.; Leising, G.; Kunert, B.; Salzmann, I.; Oehzelt, M.; Koch, N.; Vollmer, A.; Duhm, S.; Werzer, O.; Gbabode, G.; Sferrazza, M.; Geerts, Y. Crystallisation kinetics in thin films of dihexyl-terthiophene: the appearance of polymorphic phases. *RSC Adv.* **2012**, *2* (10), 4404−4414.
(27) Nečas, D.; Klapetek, P. Gwyddion: an open-source software for SPM data analysis. *Cent. Eur. J. Phys.* **2012**, *10* (1), 181−188.
(28) Shankland, N.; Florence, A. J.; Cox, P. J.; Sheen, D. B.; Love, S. W.; Stewart, N. S.; Wilson, C. C. Crystal morphology of ibuprofen predicted from single-crystal pulsed neutron diffraction data. *Chem. Commun.* **1996**, *7*, 855−856.
(29) Schrank, S.; Kann, B.; Saurugger, E.; Ehmann, H.; Werzer, O.; Windbergs, M.; Glasser, B. J.; Zimmer, A.; Khinast, J.; Roblegg, E. Impact of drying on solid state modifications and drug distribution in ibuprofen-loaded calcium stearate pellets. *Mol. Pharmaceutics* **2014**, *11*, 599−609.
(30) Yang, Z. H.; Clough, A.; Lam, C. H.; Tsui, O. K. C. Glass transition dynamics and surface mobility of entangled polystyrene films at equilibrium. *Macromolecules* **2011**, *44* (20), 8294−8300.
(31) Yang, Z. H.; Fujii, Y.; Lee, F. K.; Lam, C. H.; Tsui, O. K. C. Glass transition dynamics and surface layer mobility in unentangled polystyrene films. *Science* **2010**, *328* (5986), 1676−1679.
(32) Costa, P.; Sousa Lobo, J. M. Modeling and comparison of dissolution profiles. *Eur. J. Pharm. Sci.* **2001**, *13* (2), 123−133.